



Iranian Research Organization
for Science and Technology
(IROST)

Advances
Environmental
Technology



Journal home page: <https://aet.irost.ir>

Phenol-Contaminated Water Treatment Using Clay Nano Particles in Continuous and Batch Process and Survey the Factors Affected

Erfan Nabavi ^{a*}, Taghi Ebadi ^b, Ghorban Ali Dezvareh ^c, Mehdi Alibaglouei ^d

^a Faculty of Civil Engineering, K.N. Toosi University of Technology, Tehran, Iran.

^b Faculty of Geo-Environmental Engineering, Amir Kabir University, Tehran, Iran.

^c Faculty of Engineering, MehrAlborz University, Tehran, Iran.

^d Department of Biological Sciences, University of Cincinnati, Cincinnati, Ohio, USA.

ARTICLE INFO

Document Type:
Research Paper

Article history:
Received 26 October 2023
Received in revised form
10 May 2024
Accepted 14 June 2024

Keywords:
Phenol
Wastewater Treatment
Modified Nanoclay, HDTMA
Adsorption Process

ABSTRACT

Phenols and their derivatives are aromatic compounds containing hydroxyl or sulfonic groups attached to a benzene ring structure. Even in low concentrations, phenols are hazardous pollutants posing a threat to living organisms. This study explored the removal of phenol utilizing nano clay modified with hexadecyltrimethylammonium (HDTAM) cations. The research was conducted in three phases. The first phase involved batch experiments to eliminate phenol from aqueous solutions. In the second phase, modified nano clay was applied in a continuous system for practical purposes, investigating the impact of varying clay concentration and weight in the adsorption column. The third phase focused on studying the performance of columns in series. The results from the initial phase indicated equilibrium between the solution and adsorbent after approximately one hour, a significant reduction compared to the unmodified nano clay. Increasing the initial concentration of phenol from 50 to 800 milligrams per liter led to enhanced adsorption capacity but decreased removal efficiency from 70% to 45%. Kinetic studies revealed a pseudo-second-order adsorption process; isotherm studies indicated adherence to both the Langmuir and Freundlich models, with greater conformity to the Freundlich isotherm. The adsorption-separation model derived from the experiments suggested surface adsorption as the primary process at low concentrations, transitioning to dominant separation with increasing concentration. The second phase demonstrated the effective performance of modified clay in continuous processes, with higher flow rates resulting in reduced efficiency and adsorption capacity of phenol. Utilizing the modified clay in the adsorption column increased the phenol adsorption capacity and efficiency from 14.5% to 27%. Finally, employing two columns in series in the third phase boosted adsorption capacity from 37% to 50%.

*Corresponding author Tel.: +98 9386192129

E-mail: erfannabavi.en@gmail.com

DOI: 10.22104/AET.2024.6557.1796

COPYRIGHTS: ©2024 Advances in Environmental Technology (AET). This article is an open access article distributed under the terms and conditions of the Creative Commons Attribution 4.0 International (CC BY 4.0) (<https://creativecommons.org/licenses/by/4.0/>)

1. Introduction

One of the consequences of rapid industrial development is the production of large volumes of wastewater, resulting in the contamination of surface and groundwater resources with various organic and inorganic chemical substances, such as phenolic compounds, dyes, and heavy metals [1,2]. Phenol, in particular, is considered one of the most common organic pollutants due to its toxicity, even at low concentrations, and its potential to form byproducts through oxidation and other processes during wastewater treatment. Approximately six million tons of phenol are produced each year globally. Phenol and its derivatives are aromatic molecules that contain hydroxyl, methyl, amide, or sulfonic groups attached to a benzene ring structure [3,4]. Phenol is classified as an important pollutant in wastewater treatment due to its abundant use in various industries, including refineries, steel manufacturing, and petrochemical, ceramic, and phenolic resin industries [5]. These resins have a wide range of applications in the production of automotive materials, epoxy resins, adhesives, and polyamides. Phenol and its derivatives are present in wastewater from various industries, such as resin and plastic, olive oil production processes, textile and leather factories, casting processes, paper and pulp mills, and rubber recycling factories [6–8]. Phenol is primarily discharged into the environment through the wastewater of these industries and can have harmful effects on human health and the environment due to its toxic nature. Phenol is soluble in water and can easily migrate, which increases the likelihood of its entry into downstream water sources [9,10]. The use of phenol-contaminated water can lead to protein degradation, tissue corrosion, central nervous system impairment, as well as damage to the kidneys, liver, and pancreas [11]. Therefore, the issue of phenol-containing wastewater has become a challenging problem in water and wastewater treatment due to its high volume and pollution load [12,13]. Even at low concentrations, phenol and phenolic compounds pose a significant risk to living organisms and are classified as hazardous pollutants according to EPA and WHO standards [14,15]. The permissible limit for phenol concentration in drinking water is less than 1

milligram per liter. Reported concentrations of phenol around 2 mg/L have caused fish toxicity, and concentrations ranging from 10 mg/L to 100 mg/L have resulted in the death of aquatic organisms within 96 hours [16,17]. Furthermore, phenol has high solubility, low ionization capacity, and low vapor pressure. After oxidation and polymerization, phenol can exist as humic acid in aquatic and soil environments, complicating water and soil treatment processes [18–20].

In recent years, significant attention has been given to removing phenol and phenolic compounds using various organic compounds. Today, various treatment methods have been developed for the removal of phenol from polluted waters: surface adsorption; chemical, photocatalytic, and electrochemical oxidation; and biological and ozone processes [11,21–23]. Adsorption-based processes are one of the common methods for phenol removal. Although they have some drawbacks like other methods, they have advantages, such as low initial cost, simple design, easy operation, and insensitivity to toxic substances [24,25]. Currently, adsorption processes are widely used in water and wastewater treatment in many countries. In recent years, clay minerals have gained significant attention from researchers as adsorbents due to their affordability, abundance, and environmental compatibility [26]. Clays play an important role in controlling pollution caused by a wide range of pollutants due to their adsorption capacity and immobilization of contaminants [27–29]. The important properties of clay minerals, such as high specific surface area, layered structure, and swelling capacity, have made these materials beneficial in environmental remediation [30,31].

In this research, an attempt has been made to modify the structure of clay minerals to convert them into suitable adsorbents for the adsorption of non-ionic nonpolar organic compounds (NOCs). Nano clays have been extensively utilized due to their widespread availability, affordability, excellent adsorption capabilities, and efficiency in removing impurities. Numerous researchers have endeavored to enhance the adsorption characteristics of bentonite by optimizing its surface area, pore size, and pore volume while also considering the advantages and disadvantages of

other types of clay minerals. The improvement techniques typically involve acid treatment, treatment with both organic and inorganic compounds, and calcination, which effectively boost the surface area, porosity, and adsorption capacity of the nano clay. Nano clay is broadly classified into two, three, and four layers. The unique features of clay are high surface area, high stability, porosity, ion exchange capacity, good thermal properties, and good adsorption power. Because of these properties, clay has been exploited in many fields as catalysts and adsorbents. On the other hand, the nano clay particles can be separated by gravity procedures after the adsorption process and will no longer be stable. With the ultimate aim of enhancing the adsorption characteristics of nano clay, the main objective of this study was to investigate the use of modified nano clay (organic clay) as an adsorbent for phenol removal from aqueous solutions. In the first phase, phenol removal was examined using a batch method to understand the kinetics and isotherm of phenol adsorption by nano clay. Then, based on the information obtained from the first phase, the conditions of sand-clay filtration were determined in the second phase, and the phenol removal process was studied in a continuous system. The aim of this phase was to observe the performance of nano clay in treating phenolic solutions. In the third phase, considering the results of the second phase, a series system consisting of two identical columns containing the same amount of adsorbent was used for phenol removal. The objective of this phase was to compare the performance of single systems with series systems.

2. Materials and method

2.1. Instrumental analysis

The instruments used for measuring variables and material properties in this study included an SM shaker, a Hettich/EBA21 centrifuge, an HACH.DR4000 spectrophotometer, and a Siemens D5000 XRD for system agitation in batch experiments, removal of suspended particles,

measurement of colorant concentration, and characterization of adsorbent morphology, respectively. The phenol used in the experiments was manufactured by Merck, Germany. Some specifications of the phenol used are presented in Table 1.

2.2. Theory and method

The measurement of phenol concentration in this study was performed using a spectrophotometer based on the Stoller light absorption method. According to the Beer-Lambert law, the absorption is proportional to the concentration, meaning that as the phenol concentration increases, the light absorption also increases. The Beer-Lambert law [32] is expressed by Equation 1.

$$\log \frac{I_{in}}{I_{out}} = ABS = \epsilon LC \quad (1)$$

where I_{in} is the incident radiation, I_{out} is the transmitted radiation, ABS is the absorption at the phenol's wavelength (λm), ϵ (epsilon) is the molar absorptivity, L is the path length of the cell (cm), and C is the concentration of the substance (molarity (M)). Assuming L is constant, meaning the path length of the cell is constant, the equation can be expressed as Equation 2.

$$ABS = KC \quad (2)$$

In this equation, K is a constant value [33]. Therefore, the calibration formula for phenol could be derived by preparing several samples containing specific concentrations of the colorant and using the measured absorption values obtained by the spectrophotometer. The maximum wavelength of phenol, λm , was equal to nm270, which was obtained using the HACH DR/4000 spectrophotometer located at Amirkabir University. The pH range within the measured limits did not have an effect on the value of λm . Therefore, the absorption measurements of all samples were performed at λm . Based on this information, the relationship between the phenol concentration (mg/L) and light absorption (ABS) was determined using several samples containing specific concentrations of phenol.

Table 1. Specifications of the phenol.

Chemical Name	Chemical Formula	Solubility in Water	Max Wavelength	pKa	Density
Phenol	C ₆ H ₅ OH	83 g/L	270 nm	9.95	1.07 g/cm ³

The amount of phenol absorbed by the adsorbent in batch experiments (q_e) was calculated using Equation 3 [34].

$$q_e = \frac{(C_0 - C_e)V}{m} \quad (3)$$

where C_0 (mg/L) represents the initial concentration of phenol, C_e represents the equilibrium concentration of phenol, V (L) represents the volume of the solution, and m represents the mass of the adsorbent.

Equation 4 can be used to determine the partitioning and surface adsorption coefficients K_p and

K_{oc} , respectively, and to obtain the fractional uptake:

$$Q_p = K_{oc}f_{oc}C_e \quad \text{or} \quad Q_p = K_pC_e \quad (4)$$

The amount of uptake resulting from surface adsorption can be calculated using Equation 5:

$$Q_p = a \ln C_e + b - K_pC_e \quad (5)$$

In order to investigate the effects of changing conditions on the phenol removal behavior by the modified nano clay, certain quantities need to be calculated, which will be discussed below. To calculate the maximum adsorption capacity of phenol in the column, Equation 6 can be used:

$$q_{total} = \int_{V=0}^{V=total} (C_0 - C)dV \quad (6)$$

where C_0 represents the initial concentration, C represents the effluent concentration, and q_{total} is the maximum adsorption capacity. The equilibrium adsorption concentration, which is the amount adsorbed per unit weight of adsorbent (mg/g), can be calculated using Equation 7:

$$q_{eq} = \frac{q_{total}}{X} \quad (7)$$

where X is the total weight of the dry modified nano-clay (g). The total amount of passed phenol, W_{total} , through the column can also be calculated using Equation 8:

$$W_{total} = C_0 * V_{total} \quad (8)$$

where V_{total} is the total volume of the passing flow. The removal efficiency of phenol in the continuous system can also be calculated using Equation 9:

$$Y = \frac{q_{total}}{W_{total}} \times 100 \quad (9)$$

The successful design of a continuous system requires predicting the concentration-time profile or breakthrough curve of the effluent flow. The Thomas model is one of the most widely used models by researchers for predicting the breakthrough curve. It is used to calculate the adsorption constant and the solid-phase concentration of adsorbed phenol in the continuous system. This model is based on second-order reaction kinetics and assumes the Langmuir isotherm. The Thomas equation 10 is expressed as follows [35]:

$$\frac{C_t}{C_0} = \frac{1}{1 + \exp\left(\frac{k_{Th}}{Q}\right)(q_0X - C_0V_{eff})} \quad (10)$$

In this equation, k_{Th} represents the Thomas constant (mL/min.mg), q_0 is the maximum adsorption capacity of phenol (mg/g), and V_{eff} is the effluent flow volume in liters. The linear form of the Thomas equation 11 can be rewritten as follows:

$$\ln\left(\frac{C_0}{C_t} - 1\right) = \frac{k_{Th}q_0X}{Q} - \frac{k_{Th}C_0V_{eff}}{Q} \quad (11)$$

According to Equation 11, k_{Th} and q_0 can be obtained by plotting the $\ln(C_0/C_t-1)$ against V_{eff} .

2.3. Correction of nano clay

The correction of nano clay was performed to enhance its water repellency and increase its adsorption capacity for NOCs. To initiate the correction process, bentonite was prepared using the hydrocyclone method based on sequential sedimentation. After drying, it was milled and sieved to obtain a 200-mesh size for correction. For the correction process, montmorillonite clay was dispersed in deionized water and mechanically agitated using a mechanical stirrer. A solution containing active organic cations, equivalent to twice the clay's capacity, was gradually added to the clay suspension. The agitation was continued for six hours, followed by three rinses with distilled water. The resulting mixture was then dried and milled.

According to research conducted by scientists, it has been determined that hexadecyl trimethyl ammonium bromide (HDTMA) exhibits a greater tendency to exchange with existing cations in clays

compared to other substances. Therefore, this substance is among the most commonly used surfactants in scientific studies [36,37]. Consequently, the cation used for correction in this research is hexadecyl trimethyl ammonium bromide (HDTMA). After the correction of the clay, X-ray diffraction (XRD) analysis was employed to measure the changes in the morphological properties of the clay before and after correction. Figure S1 (**Supplementary Information**) represents the XRD pattern of the uncorrected nano clay and its constituent materials.

Batch adsorption kinetics experiments were conducted to determine the adsorption kinetics of phenol using the corrected clay. For this purpose, Erlan CC100 vials containing the required amount of phenol solution at a specific concentration were utilized along with a predetermined quantity of the adsorbent. The suspension was mixed using a shaker to ensure proper mixing. Subsequently, the suspension was centrifuged at 4000 rpm for 30 minutes using a centrifuge. Following centrifugation, the phenol concentration was measured using a spectrophotometer.

2.4. Batch adsorption isotherm experiment

In order to determine the adsorption isotherm in the laboratory, environmental parameters, such as temperature (within the range of 3 ± 25 degrees Celsius), were kept constant. The following steps were followed to obtain the equilibrium adsorption data:

- 1- Preparation of phenol solutions with specific concentrations ranging from 50 to 1000 milligrams per liter.
- 2- Adding a predetermined and equal amount of the adsorbent to all solutions.
- 3- Agitating all mixtures under consistent environmental and time conditions.
- 4- Separating the adsorbent from the suspension and analyzing the sample.

After completing the aforementioned steps and obtaining the equilibrium concentrations, adsorption isotherm plots were constructed. Then, adsorption isotherm models were fitted to the data, and adsorption parameters were determined. In this study, two isotherm models, namely Langmuir and Freundlich, were utilized.

2.5. Continuous flow experiment

To investigate phenol removal in a semi-industrial continuous flow system, a column with a diameter of 10 centimeters and a length of 0.5 meters was utilized. In this system, a centrifugal pump was used for injecting the solution into the column. Flow rate and pressure control within the column were achieved using a flowmeter and a pressure gauge, respectively. For each experiment, the column was packed with a mixture of sand and gravel in a ratio of 1:10. Additionally, all experiments were conducted at ambient temperature within the range of 2 ± 25 degrees Celsius. It is worth mentioning that experiments were also conducted to assess the adsorption of phenol by the sand, which indicated the lack of phenol adsorption by the sand.

2.6. Investigation of parameters affecting the phenol removal efficiency

In this section, the phenol removal efficiency using organic modified nano clay and the factors influencing it in the batch process will be investigated. One parameter was varied while the others were kept constant to investigate the effect of different parameters on the adsorption process. Furthermore, the kinetics and isotherms of adsorption were examined. The aim of this phase was to understand the performance of modified nano clay in relation to phenol removal. For this purpose, the factors that needed further investigation in the next phase were studied.

3. Results and Discussion

3.1. Clay modification

Figure S2 (**Supplementary Information**) illustrates the XRD analysis of the nano clay before (a) and after (b) modification. As shown in Figure S2, the XRD peak has shifted towards the left, ranging from an angle of 7 degrees to 2.3 degrees. According to Table S1 (**Supplementary Information**), the interlayer spacing has increased from 12 angstroms to 37 angstroms.

It should be noted that the substituting cations can arrange themselves in four different configurations within the interlayer spacing, depending on the degree of increase in the interlayer spacing. This arrangement of cations in the interlayer space is in a paraffinic manner. Furthermore, the surface

characteristics of the nano clay also changed after modification, transitioning from water-friendly to water-repellent.

3.2. Effect of contact time on phenol removal

To observe the effect of contact time on phenol removal, 50 mL of phenol solution (100 mg/L) was placed in contact with 0.25 g of modified nano clay in a 100 mL Erlenmeyer flask. The suspension was shaken using a shaker apparatus. It should be noted that the initial pH was 7.6. Figure 1 illustrates the effect of contact time on phenol removal efficiency. According to the figure, with an increase in contact time, the concentration of phenol in the solution decreased, and on the other hand, the removal efficiency increased. Furthermore, the adsorption process reached equilibrium with more than 80% removal efficiency in less than 1 hour. The optimal time for phenol removal could be considered to be approximately 1 hour. The high initial adsorption rate in the early minutes was due to the abundance of adsorption sites and the high driving force.

Banat et al. [36] investigated the adsorption of phenol by untreated clay. According to their reports, it took about six hours to reach equilibrium in the phenol adsorption process using untreated clay. However, based on the results obtained in this study with the modified clay, this time has been reduced to approximately one hour.

3.3. The effect of initial concentration on phenol removal efficiency

To investigate the effect of initial concentration on phenol removal efficiency, 50 milliliters of phenol solution with concentrations ranging from 50 to 800 mg/L were brought into contact with 0.25 grams of modified nano clay. The results are shown in Figure 2; the phenol removal efficiency decreased with an increase in the initial concentration. At an initial concentration of 50 mg/L, the process efficiency was over 70%, while at an initial concentration of 800 mg/L, the process efficiency dropped to less than 50%. This trend can be attributed to the saturation of active sites for adsorption at higher concentrations and a higher ratio of adsorption sites to adsorbate molecules at lower concentrations. Additionally, the increase in concentration led to an increase in the amount of phenol adsorbed per unit mass of adsorbent (Q).

This increase was due to the higher driving force at higher concentrations, resulting in more phenol being adsorbed by a fixed mass of the adsorbent. Studying the effect of initial phenol concentration in the adsorption process could provide an estimation of the adsorbent capacity for treating industrial wastewater effluents.

Banat et al. also conducted studies on phenol removal using unmodified clay, indicating a decrease in phenol removal efficiency with an increase in the initial phenol concentration. However, the slope of the reduction in phenol removal efficiency decreased with the modification, indicating an enhanced adsorption capacity of the modified clay for phenol removal [36].

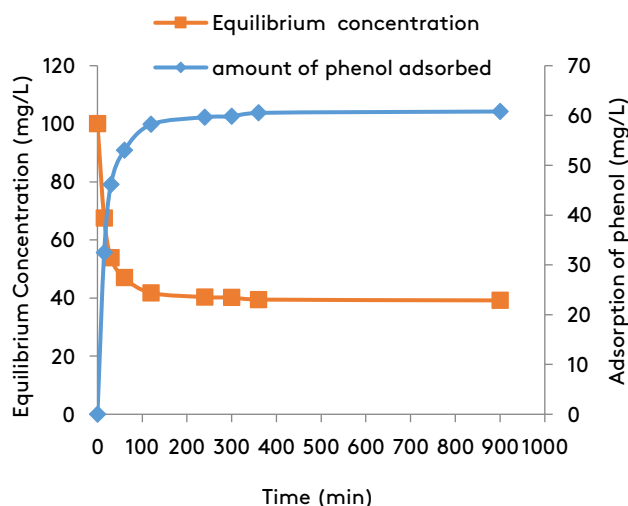


Fig. 1. The effect of contact time on adsorption of phenol by modified nano clay with (HDTMA).

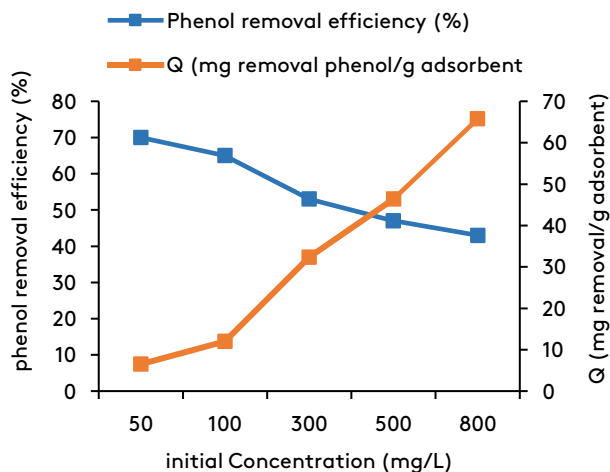


Fig. 2. The effect of initial concentration on phenol removal efficiency by HDTMA-modified nano clay.

3.4. Kinetics of phenol removal by modified nano clay with (HDTMA)

To investigate the kinetics of phenol removal, several samples of 50 mL phenol solution with a concentration of mg/L 100 were mixed with 0.25 g of modified nano clay, and the suspensions were analyzed at different time intervals. Pseudo-first-order, pseudo-second-order, and intraparticle diffusion models were fitted to the experimental data. The results are presented in Figure S3 (Supplementary Information) and Table 2. The pseudo-first-order and pseudo-second-order kinetic models were unable to identify intraparticle diffusion. Therefore, in general, the transfer from the liquid phase to the solid phase in the adsorption phenomenon could occur through mass transfer, external mass transfer, intraparticle diffusion, or a combination of these processes [38]:

- 1- Transfer from the liquid phase to the external surface of the adsorbent material.

- 2- Infiltration of the fluid into the defects and micropores of the adsorbent at the external surface.
- 3- Adsorption from the liquid phase on the internal surfaces, pores, and cavities of the adsorbent.

In this model, the intercept from the origin, denoted as l , represents the presence of other processes controlling the reaction rate in addition to intraparticle diffusion. If l is equal to zero, then only intraparticle diffusion is the controlling rate process [39,40].

Based on the R^2 values, it could be concluded that the adsorption frequency follows pseudo-second-order kinetics. On the other hand, considering the value of parameter l in the intraparticle diffusion model, it could be inferred that other processes, in addition to intraparticle diffusion, affected the adsorption of phenol by the modified nano clay, although the results showed a weak adherence to this model due to the R^2 values.

Table 2. Kinetic parameters of phenol adsorption by modified nano clay.

R^2	$q_{\text{calculated}}$	$q_{\text{experimental}}$	Model parameter	kinetic model
0.97		2.7	11.9	$K_1=0.0071s^{-1}$ Pseudo-first-order kinetics
0.99		12.5	11.9	$K_2=0.089$ $(\text{mg/g.min})^{-1}$ Pseudo-second-order kinetics
0.57		-	11.9	$K_i=0.327, l=5.49$ Interstitial diffusion kinetics

Table 3. Parameters of phenol adsorption isotherm by modified nano clay with (HDTMA)

Langmuir				Freundlich		
q_{max} (mg/g)	K_l	R_l	R^2	n	K_f (L/g)	R^2
111.1	0.004	0.21	0.973	1.52	1.08	0.996

3.6. Isotherm of phenol adsorption by modified nano clay with (HDTMA)

To study the adsorption isotherm of phenol by modified nano clay, solutions containing phenol with concentrations ranging from 50 to 800 mg/L were mixed with a constant amount of 0.25 grams of the adsorbent. In order to design a continuous system, the required parameters could be obtained by fitting two models: Langmuir and Freundlich. These two models have been widely used in previous studies, and they were also employed in this

research to investigate the adsorption isotherm of phenol. The experimental data were fitted to the Langmuir (A) and Freundlich (B) isotherm models, and the results are presented in Table 3 and Figure S4 (Supplementary Information). Based on the values of R^2 and Figure S4, it could be concluded that both models effectively described the adsorption process. The conformity of these two models indicated the presence of both monolayer adsorption and heterogeneous surface adsorption under the experimental conditions. However, the adsorption isotherm of phenol by modified nano

clay showed a better fit to the Freundlich model. According to the dimensionless constant of the Langmuir model (RI), the reaction could be classified into four situations: $0 < RI < 1$: In this case, the adsorption process was desirable. $RI > 1$: In this case, the adsorption process was undesirable. $RI = 1$: In this case, the adsorption process was linear. $RI = 0$: This indicated an irreversible adsorption process. The obtained value of RI was 0.21, indicating the suitability of the Langmuir isotherm to describe the process. On the other hand, according to the maximum adsorption capacity (q_{max}) from Table 3, the modified nano clay showed a high adsorption capacity. The maximum adsorption of phenol by modified nano clay was found to be 111 mg/g, which was 65 times higher than the capacity of unmodified nano clay reported in previous studies by Banat et al. [36]. In the Freundlich model, the constant "n" represents the deviation of the adsorption process from linearity. If "n" is equal to one, the dominant adsorption process is chemical in nature. However, based on the values in Table 2, where the constant "n" is less than one, it could be concluded that the dominant adsorption process was physical. On the other hand, according to the studies conducted by Banata et al. [36], the dominant process in phenol adsorption by unmodified clay was both chemical

and surface adsorption. Considering these results, it could be inferred that the modification of clay with organic cations led to the predominance of the physical adsorption process.

Clay minerals modified with short-chain organic cations ($C < 10$) are often referred to as adsorbent complexes. In these types of adsorbents, surface adsorption is the dominant chemical process, which is why they have limited adsorption capacity. On the other hand, clay minerals modified with long-chain organic cations ($C > 10$) are often recognized as adsorbent complexes in which the dominant adsorption process is physical. Therefore, these modified clays do not have the limitations of the previous group. The obtained results also confirmed this observation. Based on the above information, it could be concluded that clays modified with long-chain organic cations have a high capacity for adsorbing nonpolar non-ionic pollutants due to the predominance of the physical adsorption process, which is unlimited in nature.

3.7. The adsorption/partitioning model

The partitioning and surface adsorption coefficients (K_P and K_{oc}) for phenol adsorption by organic nanoclay were determined using the values provided in Table 4.

Table 4. Linear isotherm and partitioning coefficients for phenol adsorption by organic nanoclay.

K_P	K_{oc}	f %	Saturation Adsorption Capacity (mg/g)	R^2	Fitted Linear Equation	Pollutant
125	0.059	20.8	11.58	0.988	$Q_T = 0.12C_e + 19.58$	phenol

Table 5. Equations for surface adsorption and fractionation uptake of phenol by organic modified nano clay.

Equation for Surface Adsorption mg/g	Equation for Fractionation Uptake mg/g	Pollutant
$Q_A = 18.97 \ln C_e - 55.17 - 0.12 C_e$	$Q_P = 0.12 C_e$	phenol

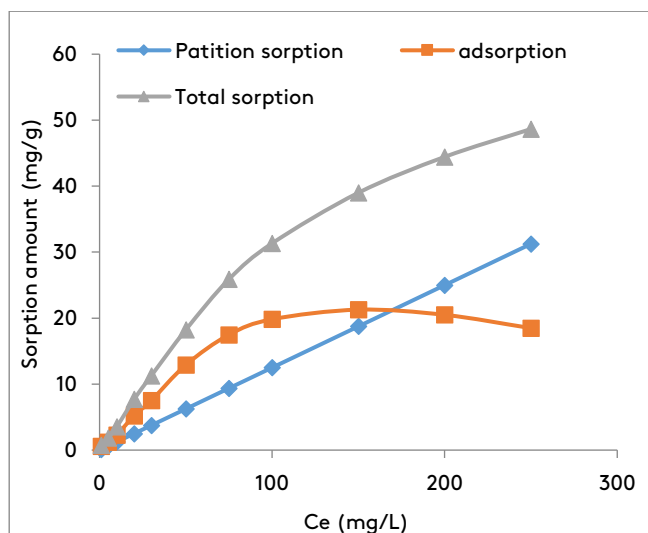


Fig. 3. Plots of the contribution of fractionation uptake and surface adsorption to the total phenol adsorption by organic modified nano clay

The equations related to the contribution of fractionation uptake and surface adsorption are presented in Table 5. The plots of QT, QA, and QP against Ce based on the model equations for phenol adsorption are shown in Figure 3.

Based on Figure 3, fractionation uptake increased linearly with increasing concentration, while surface adsorption increased nonlinearly with increasing concentration. Furthermore, surface adsorption was the dominant uptake process at

low concentrations, but its rate decreased with increasing concentration. On the other hand, due to the limited fractionation uptake capacity, its effect gradually became more significant with increasing concentration and became the dominant process in uptake. It is clear that at low concentrations, total uptake was mainly influenced by surface adsorption, while at high concentrations, fractionation uptake had a significant impact.

3.8. Evaluation of phenol removal efficiency in the continuous system (second phase)

In the second phase, the phenol removal process was investigated in a continuous system. In this phase, the effect of factors, such as flow rate and sand-to-clay ratio in the sand-clay filter, on the phenol removal process was examined. The design of continuous industrial systems requires information such as concentration-time breakthrough curves under different conditions. Additionally, parameters such as maximum adsorption capacity, percentage removal, etc., need to be determined. Therefore, the behavior of the modified nano clay in phenol adsorption should be studied under various conditions, such as changes in flow rate and other factors that may affect adsorption in the continuous system.

Table 6. Calculated parameters and Thomas constants at different flow rates (adsorbent weight g20, phenol solution concentration mg/L50).

R ²	Inlet pressure (mm Hg)	Outlet pressure (mm Hg)	W _{total} (mg)	q _{total} (mg)	q _{eq} (mg/g)	Efficiency (%)	k _{Th} (mL/min.mg)	q ₀ (mg/g)	Flow Rate (L/h)
0.96	30	80	2000	743.5	17.1	38	0.28	13.05	8
0.95	40	110	2000	470	10.7	24	0.48	6.08	15
0.97	80	145	2000	314	6.7	16	0.81	1.2	22.5

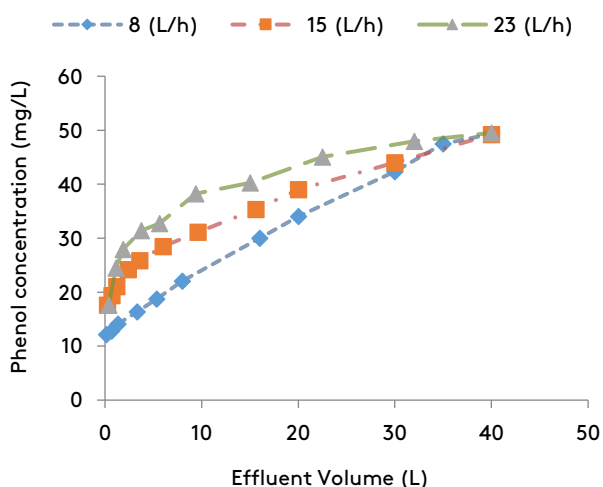


Fig. 4. The effect of flow rate on the breakthrough curve (adsorbent weight 20 g, phenol solution concentration 50 mg/L).

3.9. Effect of flow rate on phenol removal efficiency

In order to investigate the effect of flow rate on the removal efficiency of phenol, a phenol solution with a concentration of 50 mg/L was injected into a column containing 40 grams of modified nano clay and 400 grams of sand at flow rates ranging from 8 to 23 L/h. The concentration-time profiles of the effluent are presented in Figure 4. As shown in Figure 4, the concentrations of all the curves increased with time and flow volume, following a similar trend. Moreover, with increasing flow rate, the concentration of the effluent increased, and the curve shifted to the right. This occurred because reaching the equilibrium state between the adsorbent and the phenol solution required approximately one hour (based on the in-situ experimental results). Therefore, increasing the flow rate reduced the contact time between the adsorbent and the adsorbate, resulting in a leftward shift of the curve. On the other hand, increasing the flow rate led to a higher volume of fluid passing through the column per unit time, causing the column to reach saturation faster due to the faster occupation of the adsorption sites.

According to Figure S5 (**Supplementary Information**), the Thomas model was fitted to the experimental data obtained from column tests. Based on the R^2 values, the Thomas model effectively described the adsorption process. Additionally, all three curves exhibited similar

changing patterns. Using the equation of the fitted line derived from the Thomas model, the model parameters and constants were calculated for different flow rates and are presented in Table 6. As shown in Table 6, an increase in the flow rate resulted in a decrease in the removal efficiency of phenol from 38% to 16% in the system. This decrease in efficiency was due to the reduced contact time between the adsorbent and the pollutant caused by the shorter residence time in the column. On the other hand, a decrease in the flow rate led to an increase in the total amount of phenol adsorbed due to the longer hydraulic retention time in the system. Furthermore, according to Table 6, the value of the Thomas constant (k_{Th}), which represents the flow rate per unit time and mass, increased with the increase in flow rate. Additionally, by changing the flow rate, the maximum phenol adsorption capacity predicted by the Thomas model was also affected. Furthermore, the predicted values of the maximum adsorption capacity by the Thomas model are slightly lower than the experimental results, which could be attributed to the presence of a separation mechanism in phenol adsorption. The HETP (Height Equivalent to a Theoretical Plate) also decreased in the system due to the swelling of the modified nano clay caused by phenol adsorption, and an increase in the flow rate further amplified this effect.

3.10. The effect of the dose of modified nano clay on phenol removal efficiency

The effect of different doses of the modified nano clay within the range of 20 to 60 grams was examined. In this study, a phenol solution with a concentration of mg/L50 and a flow rate of L/h15 was injected into the column. The results of this investigation are presented in Figure 5. Increasing the weight of the modified nano clay in the clay-sand mixture influenced the treated flow volume significantly, leading to an increase in the treated volume with higher weight. Additionally, as the weight of the clay in the clay-sand mixture increased, the adsorbent volume and the length of the adsorption column in the cylinder increased. Consequently, the concentration of the effluent decreased significantly with an increase in the weight of the clay in the column.

For further analysis, the Thomas model was fitted to the data obtained from this part of the study, as

shown in Figure S6 (Supplementary Information). Based on the R² values, the Thomas model effectively described the phenol adsorption process in the continuous system. However, as depicted in Figure S6 (a), the model failed to predict the adsorption process in the continuous system containing 20 grams of adsorbent. This could be attributed to the decreased contact time between the solution and the adsorbent in the column due to the reduced length of the clay-sand column in the cylinder. Furthermore, the plots exhibited similar trends for different doses. The parameters and constants of the Thomas model were calculated for different doses and are presented in Table 7.

According to Table 7, the removal efficiency of phenol increased from 14% to 27% with an increase in the weight of the modified nano-clay in the column. The results still indicated a high adsorption equilibrium capacity in all three experiments. The maximum adsorption capacity of phenol (q₀, q_{eq}) was influenced by the change in the weight of the organic nanoclay in the column and increased with an increase in the weight of the nano-clay. Additionally, there was some discrepancy between the predicted values of the model and the experimental values, where the experimental values exceeded the predicted values of the model.

It is worth noting that the model failed to provide accurate predictions at a dosage of 20 grams. Furthermore, it can be observed in Table 7 that the value of k_{Th} decreased with an increase in the weight of the organic nano-clay in the column, which can be attributed to the increase in column length and adsorbent weight. On the other hand, the pressure drop (head loss) in the system increased with an increase in the amount of organic nano-clay.

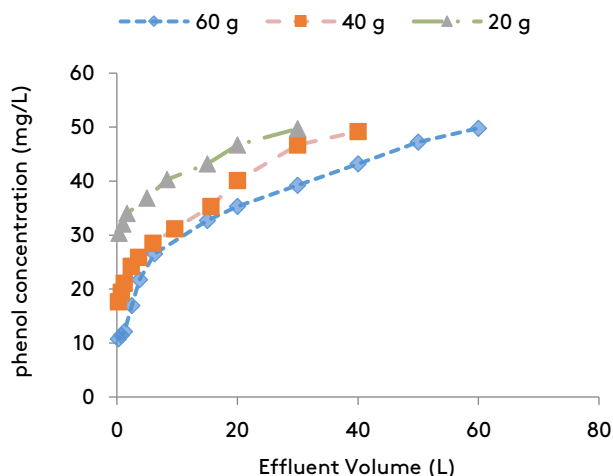


Fig. 5. The effect of adsorbent dosage on different breakthrough curves (flow rate: 20 L/h, initial phenol concentration: 50 mg/L).

Table 7. Calculated parameters and Thomas constants at different dosages (Flow Rate: L/h15, Phenol Concentration: mg/L50).

R ²	Inlet pressure (mmHg)	Outlet pressure (mmHg)	W _{total} (mg)	q _{total} (mg)	q _{eq} (mg/g)	Efficiency (%)	k _{Th} (mL/min.mg)	q ₀ (mg/g)	Adsorbent Weight (g)
-	15	80	1500	215	10.7	14.5	-	-	20
0.98	35	110	2000	493	12.34	24	0.54	5.8	40
0.92	50	140	3000	791	13.2	27	0.45	9.5	60

Table 8. The calculated and experimental values of the adsorption parameters for phenol in a series column configuration.

Columns	Flow rate(L/h)	W _{total} (mg)	q _{total} (mg)	q _{eq} (mg/g)	Removal (%)	k _{Th} (mL/min.mg)	q ₀ (mg/g)	R ²
single	8	1750	658	16.4	37	0.33	11.8	0.92
series	8	3000	1512	19.9	50.4	0.25	17.2	0.87

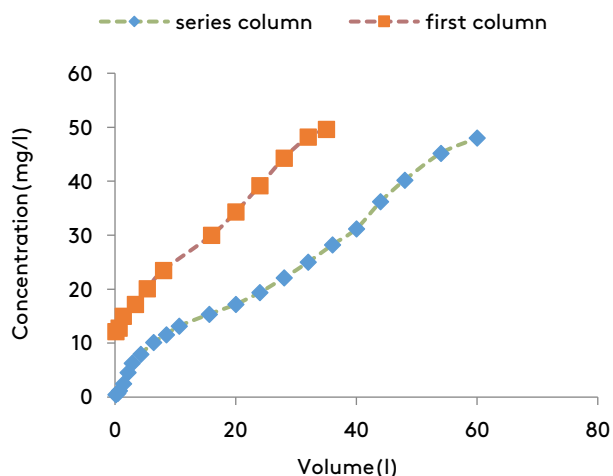


Fig. 6. The effect of adsorbent dosage on various breakthrough curves (flow rate: 15 L/h, phenol concentration: 50 mg/L).

3.11. Phenol removal in continuous series systems (Phase 3)

In the third phase, continuous series systems consisting of clay-sand filters were used to investigate the performance of the system in phenol removal. The results obtained from column studies were utilized to develop a practical system. For this purpose, two columns containing 40 grams of organic nano-clay and 400 grams of sand were connected in series. A phenol solution with a concentration of mg/L50 and a flow rate of L/h15 was injected into the columns. The results of this study are presented in Figure 6. Figure 6 clearly demonstrates that phenol was effectively removed in the series system, and the concentration of the effluent stream reached an acceptable range. Additionally, the first column reached saturation faster than the second column, which could be attributed to the higher concentration of the influent flow entering the first column. On the other hand, the saturation of the second column took longer. Furthermore, when the first column became saturated, the saturation rate of the second column increased.

Figure S7 (Supplementary Information) shows the fitting of the Thomas model to the data obtained from the series system. Based on the R² values, the Thomas model successfully described the continuous adsorption process of phenol by organic nano-clay. The calculated values of adsorption parameters and Thomas model constants are

presented in Table 8. According to Table 8, the removal efficiency of the series columns was higher compared to the single column mode. Additionally, the adsorption equilibrium capacity of phenol increased in the series system. The maximum adsorption capacity (q_0) was higher in the larger series columns. Moreover, the predicted values by the model were closer to the experimental values in the series mode. Furthermore, the value of k_{Th} in the series columns was lower than in the single column. Overall, the results indicated that the series system of clay-sand filters exhibits improved performance in phenol removal. The adsorption capacity, removal efficiency, and agreement between the model and experimental values were all enhanced in the series configuration.

4. Conclusion

In this study, the removal process of phenol using modified bentonite nanoparticles was investigated in three phases. In the first phase, the performance of the modified bentonite nanoparticles in the phenol removal process was examined in a batch system. Then, a column containing a mixture of modified bentonite nanoparticles and sand was used to study the performance of the nanoparticles in phenol removal in a continuous process. Finally, in order to achieve a more efficient system, a continuous series system with two adsorbent columns was utilized. The results obtained from the experiments indicated that the removal efficiency of phenol significantly increased with increasing contact time. After approximately one hour, the adsorption rate decreased and reached a nearly constant value. This time was about 1.6 times longer than the time required for unmodified bentonite adsorption. Furthermore, the results showed that an increase in the initial concentration of phenol led to an increase in the amount of adsorbed material per unit adsorbent mass (Q), reaching a maximum value of 111 mg/g. On the other hand, an increase in the initial concentration resulted in a decrease in the removal efficiency of phenol, ranging from 71% at a concentration of 50 mg/L to 40% at a concentration of 800 mg/L. The analysis of the results related to the pseudo-first-order and pseudo-second-order kinetics and intraparticle diffusion revealed that the adsorption process followed pseudo-second-order kinetics.

Additionally, based on the intraparticle diffusion model, it was determined that processes other than intraparticle diffusion also affected the reaction rate. The adsorption isotherm of phenol removal by modified bentonite nanoparticles was investigated using the Freundlich and Langmuir models. The results indicated a better fit to the Freundlich model. Moreover, the obtained q_{max} value from the Langmuir model indicated the successful modification of bentonite nanoparticles. On the other hand, based on the parameters of the Freundlich model, it was determined that the physical process was dominant in phenol adsorption.

The examination of the surface and pore diffusion contributions showed that at low concentrations, the surface diffusion contribution was higher than the pore diffusion contribution. However, with an increase in concentration, the surface diffusion contribution decreased until the pore diffusion became the dominant process in adsorption. The results of the flow rate variations showed that an increase in the flow rate led to a decrease in the removal efficiency of phenol from 38% to 16%. Additionally, with an increase in the flow rate through the column, the q_{eq} (mg/g) value decreased. The Thomas model was used to investigate this process, and the results confirmed the experimental findings.

The weight variations of the modified bentonite nanoparticles in the sand-bentonite mixture resulted in an increase in the phenol removal efficiency from 15% to 27%. Furthermore, an increase in the weight of the modified bentonite nanoparticles in the mixture led to an increase in q_{eq} (mg/g) from 10 to 13.5 mg/g. Moreover, an increase in the weight of the bentonite nanoparticles in the column also increased the treated flow volume. In this stage, the Thomas model was also employed to verify the obtained results. In both conducted studies in the second phase, the head loss in the system increased over time. The results obtained from using two continuous adsorption columns resulted in the reduction of phenol concentration to zero. Moreover, the q_{eq} (mg/g) value increased in the second column compared to the first column. Additionally, the phenol removal efficiency in the second column was 1.5 times higher than in the

first. Furthermore, the results indicated that with the saturation of the first column, the saturation rate of the second column increased.

Declaration of competing interest

The authors declare that they have no known competing financial interests or personal relationships that could have appeared to influence the work reported in this paper.

Data availability

The authors are unable or have chosen not to specify which data has been used.

References

- [1] Zhang, Y., Cai, P., Cheng, G., & Zhang, Y. (2022). A Brief Review of Phenolic Compounds Identified from Plants: Their Extraction, Analysis, and Biological Activity. *Natural Product Communications*, 17(1), 1934578X2110697. <https://doi.org/10.1177/1934578X211069721>
- [2] Nabavi, E., Sabour, M., & Dezvareh, G. A. (2022). Ozone treatment and adsorption with granular activated carbon for the removal of organic compounds from agricultural soil leachates. *Journal of Cleaner Production*, 335, 130312. <https://doi.org/10.1016/j.jclepro.2021.130312>
- [3] Pizani, R. S., Viganó, J., de Souza Mesquita, L. M., Contieri, L. S., Sanches, V. L., Chaves, J. O., Souza, M. C., da Silva, L. C., & Rostagno, M. A. (2022). Beyond aroma: A review on advanced extraction processes from rosemary (*Rosmarinus officinalis*) and sage (*Salvia officinalis*) to produce phenolic acids and diterpenes. *Trends in Food Science & Technology*, 127, 245–262. <https://doi.org/10.1016/j.tifs.2022.07.001>
- [4] Kisiriko, M., Anastasiadi, M., Terry, L. A., Yasri, A., Beale, M. H., & Ward, J. L. (2021). Phenolics from Medicinal and Aromatic Plants: Characterisation and Potential as Biostimulants and Bioprotectants. *Molecules*, 26(21), 6343. <https://doi.org/10.3390/molecules26216343>
- [5] Mohd, A. (2022). Presence of phenol in wastewater effluent and its removal: an overview. *International Journal of*

- Environmental Analytical Chemistry, 102(6), 1362–1384.
<https://doi.org/10.1080/03067319.2020.1738412>
- [6] Ali-Begloui, M., Salehghamari, E., Sadrai, S., Ebrahimi, M., Amoozegar, M. A., & Salehi-Najafabadi, A. (2020). Biotransformation of Trinitrotoluene (TNT) by Newly Isolated Slight Halophilic Bacteria. *Microbiology*, 89(5), 616–625.
<https://doi.org/10.1134/S0026261720050033>
- [7] Wu, P., Zhang, Z., Luo, Y., Bai, Y., & Fan, J. (2022). Bioremediation of phenolic pollutants by algae - current status and challenges. *Bioresource Technology*, 350, 126930.
<https://doi.org/10.1016/j.biortech.2022.126930>
- [8] Singh, S., Bharadwaj, T., Verma, D., & Dutta, K. (2022). Valorization of phenol contaminated wastewater for lipid production by *Rhodospiridium toruloides* 9564T. *Chemosphere*, 308, 136269.
<https://doi.org/10.1016/j.chemosphere.2022.136269>
- [9] Othmani, A., Magdoui, S., Senthil Kumar, P., Kapoor, A., Chellam, P. V., & Gökkuş, Ö. (2022). Agricultural waste materials for adsorptive removal of phenols, chromium (VI) and cadmium (II) from wastewater: A review. *Environmental Research*, 204, 111916.
<https://doi.org/10.1016/j.envres.2021.111916>
- [10] Pratyusha, S. (2022). Phenolic Compounds in the Plant Development and Defense: An Overview.
<https://doi.org/10.5772/intechopen.102873>
- [11] Mohamad Said, K. A., Ismail, A. F., Abdul Karim, Z., Abdullah, M. S., & Hafeez, A. (2021). A review of technologies for the phenolic compounds recovery and phenol removal from wastewater. *Process Safety and Environmental Protection*, 151, 257–289.
<https://doi.org/10.1016/j.psep.2021.05.015>
- [12] Panigrahy, N., Priyadarshini, A., Sahoo, M. M., Verma, A. K., Daverey, A., & Sahoo, N. K. (2022). A comprehensive review on eco-toxicity and biodegradation of phenolics: Recent progress and future outlook. *Environmental Technology & Innovation*, 27, 102423.
<https://doi.org/10.1016/j.eti.2022.102423>
- [13] Sun, J., Mu, Q., Kimura, H., Murugadoss, V., He, M., Du, W., & Hou, C. (2022). Oxidative degradation of phenols and substituted phenols in the water and atmosphere: a review. *Advanced Composites and Hybrid Materials*, 5(2), 627–640.
<https://doi.org/10.1007/s42114-022-00435-0>
- [14] Ramos, R. L., Moreira, V. R., Lebron, Y. A. R., Santos, A. V., Santos, L. V. S., & Amaral, M. C. S. (2021). Phenolic compounds seasonal occurrence and risk assessment in surface and treated waters in Minas Gerais—Brazil. *Environmental Pollution*, 268, 115782.
<https://doi.org/10.1016/j.envpol.2020.115782>
- [15] Candan Eryilmaz, & Ayten Genç. (2021). Review of Treatment Technologies for the Removal of Phenol from Wastewaters. *Journal of Water Chemistry and Technology*, 43(2), 145–154.
<https://doi.org/10.3103/S1063455X21020065>
- [16] Dezvareh, G. A., Nabavi, E., & Khodadadi Darban, A. (2022). Study of Different Microbial Corrosion Mechanisms in Sewer Pipes Network Made by Sulfur Concrete with focus on Strength and Durability Analysis. *Environmental Energy and Economic Research*, 6(4), 1–13.
<https://doi.org/10.22097/eeer.2022.344846.1255>
- [17] Adjei, J. K., Ofori, A., Megbenu, H. K., Ahenguah, T., Boateng, A. K., Adjei, G. A., Bentum, J. K., & Essumang, D. K. (2021). Health risk and source assessment of semi-volatile phenols, p-chloroaniline and plasticizers in plastic packaged (sachet) drinking water. *Science of The Total Environment*, 797, 149008.
<https://doi.org/10.1016/j.scitotenv.2021.149008>
- [18] Shamskilani, M., Niavol, K. P., Nabavi, E., Mehrnia, M. R., & Sharafi, A. H. (2023). Removal of Emerging Contaminants in a Membrane Bioreactor Coupled with Ozonation: Optimization by Response Surface Methodology (RSM). *Water, Air, & Soil Pollution*, 234(5), 304.
<https://doi.org/10.1007/s11270-023-06319-3>
- [19] Yang, Y., Zhang, P., Hu, K., Zhou, P., Wang, Y., Asif, A. H., Duan, X., Sun, H., & Wang, S. (2022). Crystallinity and valence states of

- manganese oxides in Fenton-like polymerization of phenolic pollutants for carbon recycling against degradation. *Applied Catalysis B: Environmental*, 315, 121593.
<https://doi.org/10.1016/j.apcatb.2022.121593>
- [20] Nabavi, E., Pourrostami Niavol, K., Dezvareh, G. A., & Khodadadi Darban, A. (2023). A combined treatment system of O₃/UV oxidation and activated carbon adsorption: emerging contaminants in hospital wastewater. *Journal of Water and Health*, 21(4), 463–490.
<https://doi.org/10.2166/wh.2023.213>
- [21] Nabavi, E., Sabour, M., & Dezvareh, G. A. (2021). Selection of the best leachate treatment method for the waste of leek fields using Analytic Hierarchy Process (AHP). *Advances in Environmental Technology*, 7(3), 153–170.
<https://doi.org/10.22104/aet.2021.4967.1339>
- [22] Dezvareh, G. A., Nabavi, E., Shamskilani, M., & Darban, A. K. (2023). Water Salinity Reduction Using the Phytoremediation Method by Three Plant Species and Analyzing Their Behavior. *Water, Air, & Soil Pollution*, 234(2), 90.
<https://doi.org/10.1007/s11270-023-06124-y>
- [23] Liu, T.-Y., Wang, C., Han, Y.-Z., Bai, C., Ren, H.-T., Liu, Y., & Han, X. (2022). Oxidative polymerization of bisphenol A (BPA) via H-abstraction by Bi₂15WO₆ and persulfate: Importance of the surface complexes. *Chemical Engineering Journal*, 435, 134816.
<https://doi.org/10.1016/j.cej.2022.134816>
- [24] Nabavi, E., Sabour, M., Dezvareh, G. A., & Ehteshami, M. (2023). Highly cited articles about organic leachate treatment by Fenton method in 21st century: a bibliometric and visualised analysis. *World Review of Science, Technology and Sustainable Development*, 19(3), 266–284.
<https://doi.org/10.1504/WRSTSD.2023.131930>
- [25] Stefanakis, A. I., Seeger, E., Dorer, C., Sinke, A., & Thullner, M. (2016). Performance of pilot-scale horizontal subsurface flow constructed wetlands treating groundwater contaminated with phenols and petroleum derivatives. *Ecological Engineering*, 95, 514–526.
<https://doi.org/10.1016/j.ecoleng.2016.06.105>
- [26] Awasthi, A., Jadhao, P., & Kumari, K. (2019). Clay nano-adsorbent: structures, applications and mechanism for water treatment. *SN Applied Sciences*, 1(9), 1076.
<https://doi.org/10.1007/s42452-019-0858-9>
- [27] Nabavi, E., Shamskilani, M., Dezvareh, G. A., & Darban, A. K. (2023). ANN-Based Modeling of Combined O₃/H₂O₂ Oxidation, and Activated Carbon Adsorption Treatment System: Forest Polluting Site Leachate. *Water, Air, & Soil Pollution*, 234(2), 86.
<https://doi.org/10.1007/s11270-023-06099-w>
- [28] Li, C., Zhu, N., Yang, S., He, X., Zheng, S., Sun, Z., & Dionysiou, D. D. (2021). A review of clay based photocatalysts: Role of phyllosilicate mineral in interfacial assembly, microstructure control and performance regulation. *Chemosphere*, 273, 129723.
<https://doi.org/10.1016/j.chemosphere.2021.129723>
- [29] Barakan, S., & Aghazadeh, V. (2021). The advantages of clay mineral modification methods for enhancing adsorption efficiency in wastewater treatment: a review. *Environmental Science and Pollution Research*, 28(3), 2572–2599.
<https://doi.org/10.1007/s11356-020-10985-9>
- [30] Alibagloui, M., Trutschel, L. R., Rowe, A. R., & Sackett, J. D. (2023). Complete genome sequence of *Halomonas* sp. strain M1, a thiosulfate-oxidizing bacterium isolated from a hyperalkaline serpentinizing system, Ney Springs. *Microbiology Resource Announcements*, 12(11).
<https://doi.org/10.1128/MRA.00508-23>
- [31] Sarkar, B., Rusmin, R., Ugochukwu, U. C., Mukhopadhyay, R., & Manjaiah, K. M. (2019). Modified clay minerals for environmental applications. In *Modified Clay and Zeolite Nanocomposite Materials* (pp. 113–127). Elsevier.
<https://doi.org/10.1016/B978-0-12-814617-0.00003-7>
- [32] Kolesnichenko, P. V., Eriksson, A., Lindh, L., Zigmantas, D., & Uhlig, J. (2023). Viking Spectrophotometer: A Home-Built, Simple, and Cost-Efficient Absorption and Fluorescence Spectrophotometer for Education in Chemistry. *Journal of Chemical Education*, 100(3), 1128–1137.
<https://doi.org/10.1021/acs.jchemed.2c00679>

- [33] Zollinger, H. (2003). *Color chemistry: syntheses, properties, and applications of organic dyes and pigments*. John Wiley & Sons.
- [34] Crittenden, J. C., Trussell, R. R., Hand, D. W., Howe, K. J., & Tchobanoglous, G. (2012). *MWH's water treatment: principles and design*. John Wiley & Sons.
- [35] Han, R., Zou, W., Li, H., Li, Y., & Shi, J. (2006). Copper(II) and lead(II) removal from aqueous solution in fixed-bed columns by manganese oxide coated zeolite. *Journal of Hazardous Materials*, 137(2), 934–942.
<https://doi.org/10.1016/j.jhazmat.2006.03.016>
- [36] Banat, F. A., Al-Bashir, B., Al-Asheh, S., & Hayajneh, O. (2000). Adsorption of phenol by bentonite. *Environmental Pollution*, 107(3), 391–398.
[https://doi.org/10.1016/S0269-7491\(99\)00173-6](https://doi.org/10.1016/S0269-7491(99)00173-6)
- [37] Fukushima, Y. (2005). Organic/Inorganic Interactions in Polymer/Clay Mineral Hybrids. *Clay Science*, 12(Supplement1), 79–82.
https://doi.org/10.11362/jcssjclayscience1960.12.Supplement1_79
- [38] Nethaji, S., Sivasamy, A., Thennarasu, G., & Saravanan, S. (2010). Adsorption of Malachite Green dye onto activated carbon derived from *Borassus aethiopum* flower biomass. *Journal of Hazardous Materials*, 181(1–3), 271–280.
<https://doi.org/10.1016/j.jhazmat.2010.05.008>
- [39] Chen, S., Zhang, J., Zhang, C., Yue, Q., Li, Y., & Li, C. (2010). Equilibrium and kinetic studies of methyl orange and methyl violet adsorption on activated carbon derived from *Phragmites australis*. *Desalination*, 252(1–3), 149–156.
<https://doi.org/10.1016/j.desal.2009.10.010>
- [40] Xu, X., Gao, B.-Y., Yue, Q.-Y., & Zhong, Q.-Q. (2010). Preparation and utilization of wheat straw bearing amine groups for the sorption of acid and reactive dyes from aqueous solutions. *Journal of Hazardous Materials*, 182(1–3), 1–9.
<https://doi.org/10.1016/j.jhazmat.2010.03.071>

How to site this paper:



Nabavi, E., Ebadi, T., Dezvareh, Gh. A., & Alibaglouei, M. (2024). Phenol-Contaminated Water Treatment Using Clay Nano Particles in Continuous and Batch Process and Survey the Factors Affected. *Advances in Environmental Technology*, 10(3), 202-217. doi: 10.22104/AET.2024.6557.1796